TISSUE ENGINEERING: Part C
Volume 16, Number 6, 2010

DOI: 10.1089/ten.tec.2009.0751

Application of Low-Frequency Alternating Current Electric Fields Via Interdigitated Electrodes: Effects on Cellular Viability, Cytoplasmic Calcium, and Osteogenic Differentiation of Human Adipose-Derived Stem Cells

Seth D. McCullen, Ph.D.,[1] John P. McQuilling, B.S.,[1] Robert M. Grossfeld, Ph.D.,[2] Jane L. Lubischer, Ph.D.,[2] Laura I. Clarke, Ph.D.,[3] and Elizabeth G. Loboa, Ph.D.[1]

Electric stimulation is known to initiate signaling pathways and provides a technique to enhance osteogenic differentiation of stem and/or progenitor cells. There are a variety of *in vitro* stimulation devices to apply electric fields to such cells. Herein, we describe and highlight the use of interdigitated electrodes to characterize signaling pathways and the effect of electric fields on the proliferation and osteogenic differentiation of human adipose-derived stem cells (hASCs). The advantage of the interdigitated electrode configuration is that cells can be easily imaged during short-term (acute) stimulation, and this identical configuration can be utilized for long-term (chronic) studies. Acute exposure of hASCs to alternating current (AC) sinusoidal electric fields of 1 Hz induced a dose-dependent increase in cytoplasmic calcium in response to electric field magnitude, as observed by fluorescence microscopy. hASCs that were chronically exposed to AC electric field treatment of 1 V/cm (4 h/day for 14 days, cultured in the osteogenic differentiation medium containing dexamethasone, ascorbic acid, and β-glycerol phosphate) displayed a significant increase in mineral deposition relative to unstimulated controls. This is the first study to evaluate the effects of sinusoidal AC electric fields on hASCs and to demonstrate that acute and chronic electric field exposure can significantly increase intracellular calcium signaling and the deposition of accreted calcium under osteogenic stimulation, respectively.

Introduction

The application of electric stimulation in tissue engineering provides an exciting route for cell manipulation, and considerable progress in this area has occurred as the interaction of electric fields, currents, and potentials with cells has become better understood.[1–3] Within cells and tissues, ionic currents and electric potentials exist naturally and influence cell and tissue function and development.[1,4] Disruption or alteration of ionic gradients or cell surface charges by an applied electric field can lead to changes in cell signaling pathways and gene expression, resulting in differences in differentiation, proliferation, and mobility.[3–5]

Since the discovery of the natural electrical properties of bone, the idea of coupling endogenous and exogenous electrical activity has been introduced as a possible tool to promote bone fracture healing and differentiation of osteoprogenitor cells.[6–10] Mechanical and electrical stimuli have been known for some time to affect the properties and regenerative capacity of skeletal tissues. Extremely low-frequency electric fields significantly affect stem cell populations, by enhancing cell signaling pathways and differentiation.[3,3,11] Electrical stimulation modifies the properties of multiple cell types, including the differentiation of neuronal and mesenchymal stem cells (MSCs), by modulating intracellular calcium (Ca^{2+}) signaling and augmenting tissue-specific markers.[3,11,12]

MSCs are an important therapeutic tool in the field of regenerative medicine.[13] MSCs can be derived from a range of mesodermal tissues, including bone marrow and adipose tissue. Human adipose-derived stem cells (hASCs) have gained increasing interest in the field of regenerative medicine because of their multilineage potential and relative ease of acquisition and harvest compared to other stem cell

[1]Joint Department of Biomedical Engineering at the University of North Carolina at Chapel Hill and North Carolina State University, Raleigh, North Carolina.
Departments of [2]Biology and [3]Physics, North Carolina State University, Raleigh, North Carolina.

types.[14–16] Although hASCs have been used successfully in tissue engineering, to our knowledge, there have been limited studies that have assessed the interaction of adipose-derived stem cells with electric fields. Recent work by Hammerick *et al.* assessed the response of mouse ASCs to electrical stimulation applied via ionic salt bridges and demonstrated an enhancement in early osteogenic markers, but not in terminal differentiation as measured by calcium accretion.[17]

With the relative ease of harvest and availability of stem cells such as hASCs, researchers have been striving to develop rigorous methodologies that allow for the controlled application of physical forces on stem cells to evaluate both short- and long-term effects of these stimuli. Traditional methods of exposing cells to electric fields involve capacitative coupling, semicapacitative coupling, and/or ionic salt bridges to generate the desired field and frequency pattern.[18–21] These approaches have limitations with heterogeneity in trial design, dosage, and delivery method. An alternative method is the use of interdigitated electrode (IDE) arrays. IDEs have long been used for dielectrophoresis of biological materials and cell patterning, yet the use of this configuration has not been examined for application of low frequency electric fields during culture of stem cells.[22] IDEs create an electric field both parallel to and above the surface of the electrode. Using planar IDEs for cellular electrical stimulation has the following advantages: (1) because the electrodes are rigidly fixed on the substrate, it enables highly reproducible, facile application of controlled, well-quantified electrical stimulation, (2) small electrode spacing (down to 10 μm), similar to physiological feature sizes, can be easily fabricated, and at small electrode spacing, only a low voltage is needed to create physiological electric field strengths, and (3) due to the open nature of the IDEs, cells can easily be observed during stimulation, so short-term responses (i.e., cytoplasmic calcium increase) can be directly correlated with longer-term effects (i.e., end product expression) when the cells are cultured under the same electrical stimulation.

The objectives of this study were to investigate the interaction of electrical stimulation with hASCs cultured on IDEs by (1) characterizing acute hASC responsiveness in terms of intracellular calcium signaling and viability as a function of electric field strength and (2) assessing electric field effects on the osteogenic differentiation of hASCs. The electric field frequency was 1 Hz. We hypothesized that hASCs would be more responsive to electrical stimulation at increasing field strength up to a limit when cellular viability would decrease (100 V/cm or higher), and that when exposed to a physiologically appropriate, defined alternating current (AC) electric field, hASCs would respond by enhanced calcium accretion compared to unstimulated controls.

Materials and Methods

Cell isolation and culture

Excess human adipose tissue was obtained at University of North Carolina–Chapel Hill by voluntary liposuction procedure in accordance with an approved IRB protocol (IRB 04-1622). Adipose tissue samples were harvested from the visceral abdominal region with skin flaps attached to the tissue. The skin was cut away and discarded before adipose tissue digestion. hASCs were isolated from ~50 g of adipose tissue from each donor using a method modified from Zuk *et al.* as we have previously described.[14,24] hASCs were characterized via immunohistochemical analysis as positive for surface markers CD105 and CD166 and negative for CD34 and CD45,[14] and the differentiation potential was tested during 2 weeks of culture in complete growth, adipogenic differentiating, and osteogenic differentiating media. Complete growth medium contained Eagle's Minimum Essential Medium, alpha-modified supplemented with 10% fetal bovine serum, 2 mM L-glutamine, 100 units/mL penicillin, and 100 μg/mL streptomycin. Osteogenic differentiating medium contained complete growth medium supplemented with 50 μM ascorbic acid, 0.1 μM dexamethasone, and 10 mM β-glycerolphosphate. Adipogenic differentiating medium contained complete growth medium plus 1 μM dexamethasone, 5 μg/mL insulin, 100 μM indomethacin, and 500 μM isobutylmethylxanthine. Cells were cultured initially in each of these media for 2 weeks to confirm the ability of the hASCs to differentiate down both osteogenic and adipogenic pathways. Accumulation of deposited calcium was observed using Alizarin Red S, and lipid accumulation was observed using Oil Red O (Fig. 1). hASCs were used at passages 2–3 for all experiments and underwent two freeze–thaw cycles. For all experiments hASCs were expanded in T-75 flasks for ~1 week, or to 80% confluence, and were then trypsinized, resuspended, and seeded directly onto IDEs.

IDE fabrication

Electrical stimulation of hASCs was performed by fabricating a custom setup (Fig. 2a). IDEs were fabricated utilizing conventional ultraviolet (UV) lithography techniques. They consisted of two gold contact pads, where each pad was connected to 25 "fingers" or "digits" (Fig. 2b). The spacing between digits and the digit width were both 100 μm. The diminutive spacing between the electrode fingers allowed physiologically relevant fields to be obtained with the application of low voltages, thus eliminating electrochemical effects. To produce the IDEs, glass slides with a No. 2 thickness were cleaned in UV-ozone cleaner for 30 min, spin-coated at 4500 rpm with Shipley's Microposit S1813 photoresist (Microchem), and baked for 45 min in a convection oven at 100°C. After baking, coated glass slides were exposed to UV light at 120 mW with a Cr mask with the desired IDE pattern and developed with Microposit MF (Microchem) 351 for 1 min. After residual S1813 was removed, glass slides were coated with 100 Å Cr and 1000 Å Au. Excess metal was removed and the individual electrodes were connected in parallel with biocompatible H20E EPOTEK silver conductive epoxy (Ted Pella), cured at 150°C for 5 min. Platinum wires (Cal. Fine Wire, gauge 36) were attached to the end electrodes and to connectors. Matching connectors were bonded to platinum wires that were soldered to split Bayonet Neill-Concelman connectors (BNC). Assembled electrode tissue culture flasks (Nunc) (Fig. 2a) were cleaned with N_2 gas and 70% ethanol before being sterilized with ethylene oxide (Andersen Sterilizers) (Fig. 2b). An Agilent 33220A 20 MHz Function/Arbitrary Signal generator was used at 0.01–10 V peak-to-peak stimulus intensity to generate calculated fields ranging from 1 to 1000 V/cm at a frequency of 1 Hz. The waveform and intensity were confirmed with an oscilloscope.

Electric field modeling

The electric field was modeled by approximating the potential (V) applied based on Equation 1 originally derived by den Otter,[23] using MAPLE 12 Software (Maplesoft) where V_o = applied potential, x = the distance between two electrode fingers, a = the periodicity of the finger spacing, y = the height above the plane of the electrode, s = spacing between two electrodes (100 μm), and n = the array size. As y increases, moving away from the electrode plane, the voltage decays in a nonlinear manner so that ~150 μm above the electrode, the electric field is negligible. hASCs are seeded directly on the electrode, where the electric field is essentially constant.

$$V(x,y) = \frac{4V_o}{\pi}\sum_{n=1}^{\infty}\frac{1}{2n-1} * \sin\frac{(2n-1)\pi x}{a} * exp\left(-(2n-1) * \pi * \frac{abs(y)}{a}\right) * BesselJ\left(\frac{(2n-1)\pi s}{2a}\right)$$

Acute electric field stimulation

hASCs from two Caucasian women (ages 44 and 49) were seeded at a density of 20,000 cells/cm^2. After 24 h in culture, hASCs were exposed to various acute electric field treatments 1, 10, 100, or 1000 V/cm at $f = 1$ Hz. hASC viability was determined with a Live/Dead Assay Cytotoxicity Kit (Molecular Probes) for mammalian cells. At days 2–7 of culture in complete growth medium, hASCs were imaged to examine changes in cellular cytoplasmic Ca^{2+} elicited by acute electric field stimulation. The cell-seeded electrodes were incubated 1 h at 37°C in 1 mL Hank's balanced salt solution (HBSS; Sigma Chemical) containing 0.25 μL of the vital dye Cell Tracker Red CMTPX (Invitrogen, prepared by resuspending 50 μg of dye in 50 μL dimethyl sulfoxide plus 5 μL Pluronic F-127, 20% in dimethyl sulfoxide) and 4 μL of the Ca^{2+}-sensitive dye Fluo-4 AM (Invitrogen, prepared as for the vital dye). They were then rinsed with 1 mL HBSS and incubated 30 min with 1 mL dye-free HBSS to allow Fluo-4 de-esterification for retention in the cells. The chamber was mounted on the stage of an upright Leica DMR microscope configured with fluorescence optics. A 20× HCX APO 0.50 NA water immersion objective and a mercury bulb filtered for excitation at 488 nm and emission at 530 nm (for green light from Fluo-4) or excitation at 577 nm and emission at 602 nm (for red light from the vital dye) were used to image a representative region of the hASC-seeded electrode. HBSS was pumped continuously through the chamber at a rate of 3 mL/min, initially for a control period of 5 min and subsequently for several 5 min periods of electrical stimulation with 3–10 min unstimulated intervals between. Images were captured continuously at a rate of ~1/s by a digital charge-coupled device (CCD) camera (IEEE1394; Hamamatsu Photonic Systems) and viewed in real time with Open lab software (Improvision).

Chronic electric field stimulation

hASCs were also exposed to repeated electrical stimulation to determine any long-term effects on osteogenic differentiation of hASCs cultured in osteogenic differentiating medium. Electric field treatments of 0 (control), 1, 3, and 5 V/cm at 1 Hz were applied to hASCs for 4 h/day for 14 days. These electric field values were chosen based on acute electric field stimulation results. hASCs were analyzed for cellular viability, DNA content for proliferation, and mineralized calcium content on days 7 and 14. Cell viability was determined with a Live/Dead Assay Cytotoxicity Kit (Molecular Probes) for mammalian cells. On days 7 and 14, hASC-seeded IDEs were rinsed twice in 1× phosphate-buffered saline and incubated for 20 min in 4 μM calcein AM and 4 μM ethidium homodimer-1 protected from light. Live cells fluoresced green and dead cells fluoresced red. Proliferation was determined by quantifying DNA using the DNA binding dye Hoechst 33258 in microplate format after an overnight digestion at 60°C in 2.5 units/mL papain from papaya latex in phosphate-buffered saline with 5 mM ethylenediaminetetraacetic acid and 5 mM cysteine HCl (all reagents from Sigma Chemical). Cell-deposited calcium content was determined by digesting cell-seeded electrodes in 0.5 N HCl overnight and assaying the supernatant using the Calcium Liquicolor Assay (Stanbio).

Data analysis

Experiments were performed with at least three independent trials per donor using hASCs from two different donors. Chemical assays were done in triplicate. Image Pro Plus 6.2 software (Media Cybernetics) was used to generate line graphs of the time course of changes in cytoplasmic Ca^{2+} of all individual cells in the field of view, selected manually, before and during electric field stimulation. The data were transferred into a Microsoft Excel file for quantification of the changes in cellular fluorescence in comparison with the

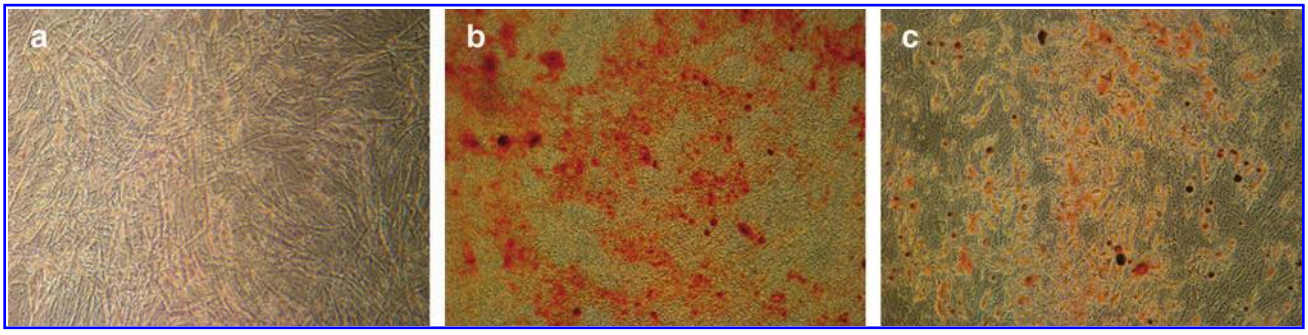

FIG. 1. Histological staining of human adipose-derived stem cells (hASCs) cultured under complete growth (**a**), osteogenic (**b**), or adipogenic (**c**) medium conditions for 2 weeks *in vitro.* hASCs cultured under osteogenic and adipogenic medium conditions stained positive for calcium deposits via Alizarin Red S or fat droplets via Oil Red O, respectively. Color images available online at www.liebertonline.com/ten.

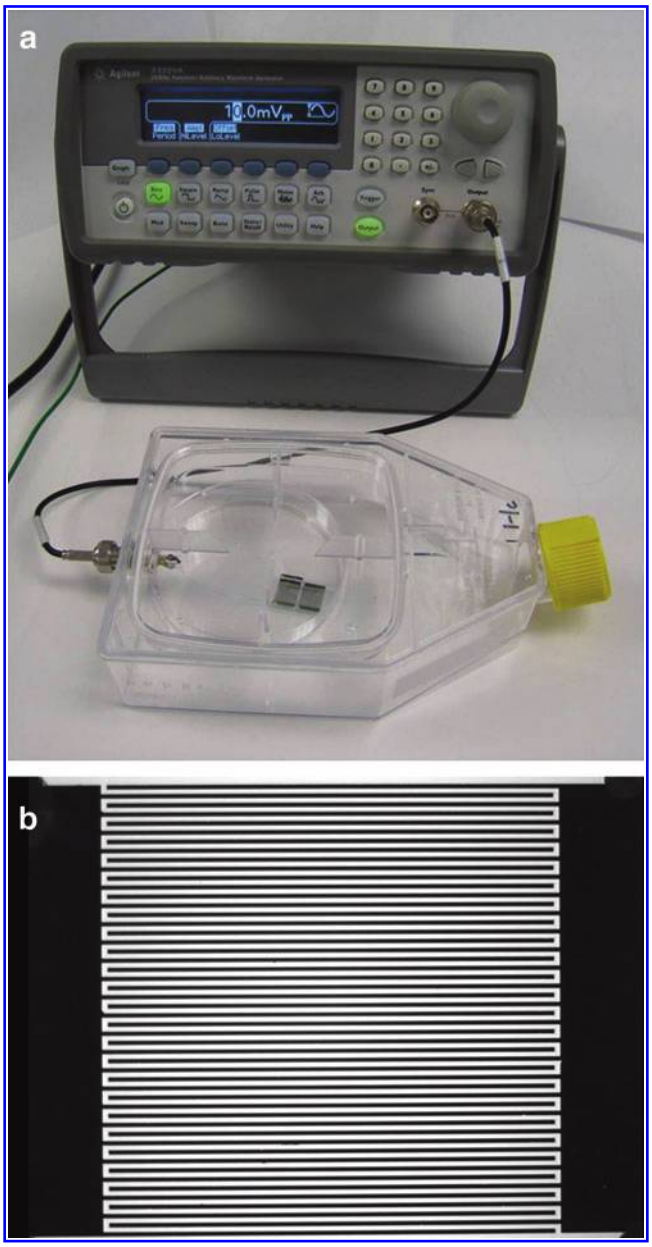

FIG. 2. Image of interdigitated electrode assembled in flask (**a**) and close-up image of interdigitated electrode showing contact pads and electrode array (**b**). The bright (white) regions are glass, whereas the dark regions are metal. Color images available online at www.liebertonline.com/ten.

initial control period preceding electrical stimulation. Quantitative data are presented as mean ± standard error of the mean. Significant differences were determined by performing Welch's *t*-tests due to unequal variances. A *p*-value < 0.05 was considered significant.

Results

hASCs were viable and morphologically normal with weak to moderate electric field stimulation

IDEs produce an electric field between the electrode fingers that also penetrates above and below the electrode. The

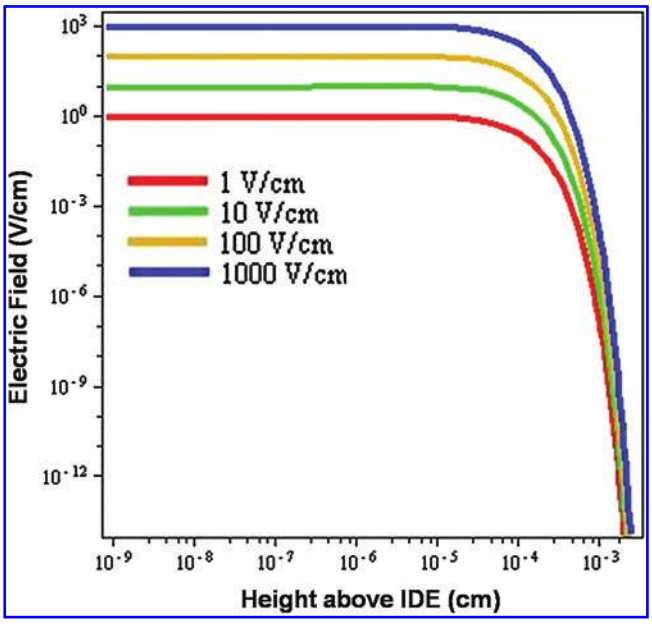

FIG. 3. Graphical depiction of electric field at different magnitudes above the interdigitated electrode plane demonstrating its exponential decay with height. Color images available online at www.liebertonline.com/ten.

height of the electric field penetration into solution can be modified by altering the electrode lithography. Figure 3 depicts the calculated electric potential at increasing height above the electrode for varying applied potentials. By increasing the applied potential between the electrode fingers, the electric field magnitude increases, correspondingly. As can be seen, the shape of the curve is independent of the field amplitude. With increasing height above the plane of the electrode, the electric field is relatively constant until it begins to decay significantly $\sim 100\,\mu m$ (one electrode spacing) above the plane of the electrode. This demonstrates that the electric field pattern is controlled by the electrode feature size, as has been previously shown,[25] rather than the applied voltage.

hASCs were able to adhere and spread on the IDE surface (Fig. 4a). Although the electrode height of the IDE was minimized ($\sim 100\,nm$) to prevent preferential alignment of hASCs along the electrode fingers, some alignment was observed (Fig. 4). In general, however, the hASCs appeared to be uniformly distributed and randomly aligned on the IDE surface (Fig. 4). hASC morphology was consistent with that on tissue culture plastic, displaying a spindly fibroblastic shape. After initial seeding, hASCs were exposed to varying electric field magnitudes for 30 min to determine any detrimental effects on cell viability (Fig. 4). With 1 and 10 V/cm stimulation at 1 Hz, which are physiological values *in vivo*, hASCs remained viable.

hASCs were disturbed by strong, protracted electric field stimulation

As the electric field increased in magnitude (stimulation for 30 min at 1 Hz), it was evident that the hASC monolayer was distorted, as hASCs were removed and a perforated interface was created. This was most apparent at 100 V/cm, where the monolayer was deformed as spherical perforations

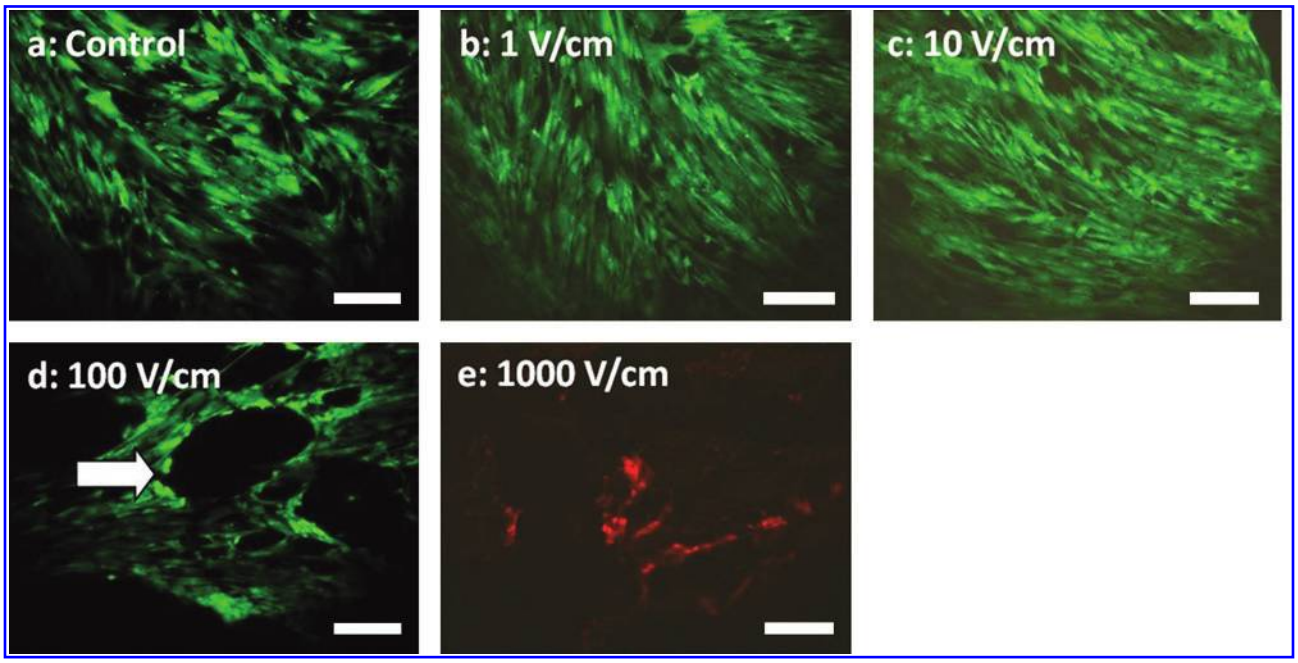

FIG. 4. Viability images of hASC-seeded electrodes after 30 min exposure to sinusoidal electric fields of 0 (control, **a**), 1 (**b**), 10 (**c**), 100 (**d**), or 1000 (**e**) V/cm at 1 Hz. hASCs were viable up to electric field magnitudes of 10 V/cm. At electric fields of 100 V/cm or higher, cell detachment was seen with large regions of cells removed from the electrode (as indicated by arrow). After exposure to 1000 V/cm at 1 Hz for 30 min, hASC viability was completely compromised. Live cells = green; dead cells = red. Scale bar = 200 μm. Color images available online at www.liebertonline.com/ten.

were formed (Fig. 4d, arrow). With 1000 V/cm stimulation for 30 min, there were virtually no viable cells present anywhere on the device (Fig. 4e). Immediately after stimulation at 1000 V/cm, the cells began to delaminate from the surface and undergo membrane breakdown via electroporation. Figure 4e displays the presence of nucleic acids (stained red) left on the IDE device under these conditions. These results, at nonphysiological field strengths, confirm that electric fields are present due to the IDE configuration, and demonstrate the types of damage possible from relatively high field strengths.

Acute electric field stimulation increased cytoplasmic Ca^{2+} in hASCs and did not compromise hASC viability

hASCs exhibited variable levels of cellular fluorescence during the initial control period (Figs. 6 and 7a) with no electric field applied. The fluorescence level varied with time depending on the cell. There was no obvious correlation between spontaneous activity and stimulus-evoked activity.

Significant increases in cellular fluorescence intensity were noted with stimulation for 1–10 min at 1, 10, and 100 V/cm, at 1 Hz (Fig. 5). This indicates that electrical stimulation caused an increase of calcium within the cells. The results were comparable for both hASC cell lines. The effect was greater at larger field strengths (Figs. 5–7). In some experiments, there was a small increase in the number of responsive cells and in their fluorescence output with stimulation at 1 V/cm (Figs. 5–7). At higher fields, most cells responded and the effect was clearly observed. The magnitude of the increase in cellular fluorescence was directly related to the magnitude of the stimulus intensity (Figs. 5–7). Figure 5 displays representative pseudocolor images of an hASC-seeded IDE, showing the hASC monolayer stained with a vital dye (Red Cell Tracker; Fig. 5a), and increases in cytoplasmic calcium with increased electric field strength (Fig. 5b–e). The cells exhibited obvious increases in cytoplasmic calcium within ~30 s of initiating stimulation at these intensities and the effects continued for the duration of the stimulation period and beyond. The rate and extent of

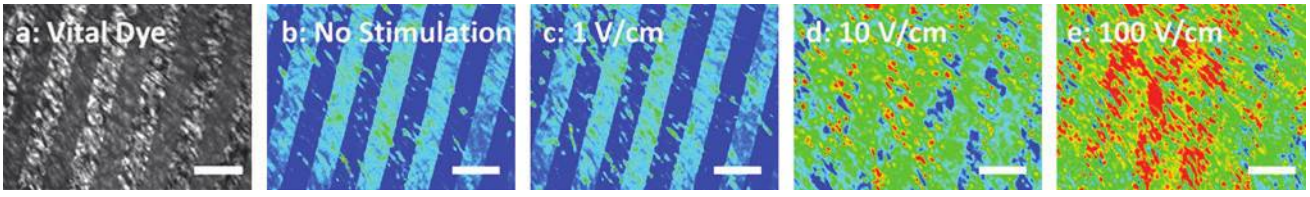

FIG. 5. Vital dye image of hASCs (**a**), and pseudocolor images of cellular fluorescence as an indicator of intracellular Ca^{2+} levels (**b–e**) immediately after electric field exposure of 0, 1, 10, or 100 V/cm at 1 Hz for 5 min. Fluorescence intensities vary from blue to red (low to high, respectively), indicating an increase in the amount of calcium present within the cells. Scale bar = 200 μm. Color images available online at www.liebertonline.com/ten.

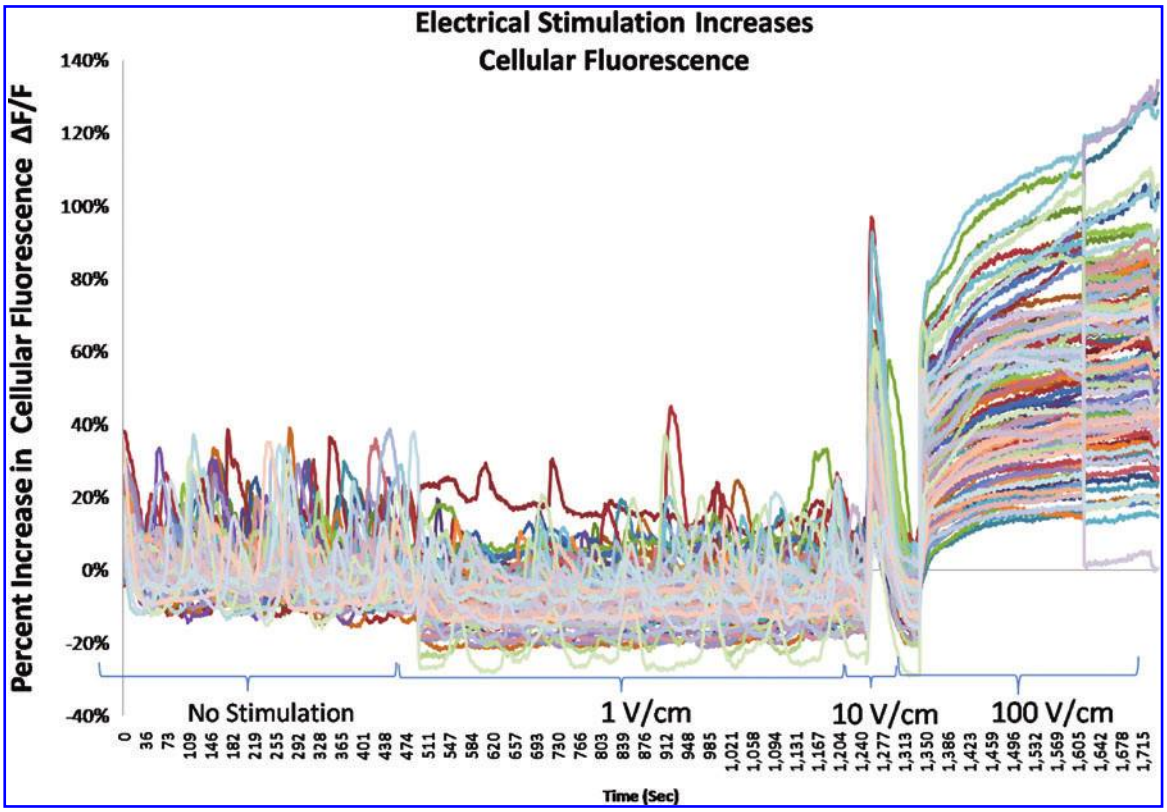

FIG. 6. Graphical representation of fluorescence intensities from all cells in the field of view in a representative experiment. Electrical stimulation increased cytoplasmic Ca^{2+}, especially at 10 and 100 V/cm as compared to the preceding unstimulated control period. Color images available online at www.liebertonline.com/ten.

increase differed between different cells and the cellular response tended to be more reproducible and predictable for samples with cells plated at higher density.

The majority of plated cells remained viable during these treatments. Even after 5 min of stimulation at 100 V/cm at 1 Hz, the majority of hASCs remained viable, as demonstrated by their lack of uptake of propidium iodide. This dye binds to DNA of damaged cells that have compromised cell membranes, which it did when the medium was acidified but not when they were electrically stimulated. In addition, when the sequence of stimulation treatments was reversed, that is, from high to low intensity (Fig. 7a), the cells continued to respond after a 100 V/cm treatment and responded to 100 μM adenosine triphosphate (ATP) with an increase in cytoplasmic calcium (not shown) much as they would have had they not been first stimulated electrically.

Chronic electric field stimulation enhanced Ca^{2+} deposition in hASCs

To determine the long-term effects of electric field stimulation on osteogenesis, hASCs were cultured on IDEs for 2 weeks in osteogenic differentiating medium and stimulated at varying electric fields of 0, 1, 3, and 5 V/cm at 1 Hz for 4 h/day up to 14 days. hASC viability remained high for all treatment groups, with few dead cells present on day 7 or 14 (Fig. 8).

hASC proliferation was assessed by measuring DNA content. On day 7, hASCs exposed to a 5 V/cm field had a significantly higher amount of DNA compared to all other treatments (Fig. 9). By day 14, cellular proliferation was not statistically different between treatment groups.

To assess osteogenic differentiation of the hASCs, mineralized calcium was quantified. There was a significant decrease in hASC mineralization for the 5 V/cm AC electric field after 7 days of stimulation relative to hASCs exposed to a 1 V/cm field (Fig. 10). By day 14, there was a significant increase in mineralized calcium for hASCs exposed to a 1 V/cm field compared to hASCs in all other treatments groups (Fig. 10). Exposure to a 5 V/cm AC field decreased the amount of mineralized calcium compared to the unstimulated control.

Discussion

A variety of techniques for electrical stimulation have proven successful in clinical and research settings, including direct probe placement within bone tissue, capacitative coupling with metal plates placed outside the culture, and application of changing magnetic fields, which induce an alternating electric field within the tissue.[26] In these approaches, AC (rather than direct current) is often utilized to prevent ion buildup near electrodes, which can negate the applied field or current. In previous work on electrical stimulation in other cell lines, electric field amplitudes in the order of 0.1–10 V/cm have been identified as sufficient to produce an effect without damage, and frequencies <15 Hz are commonly used, as aggregates of cells may act as a low-pass filter to the electrical signal.

By culturing hASCs directly on an IDE surface, we were able to expose the cells to a controlled, but intricate, pattern

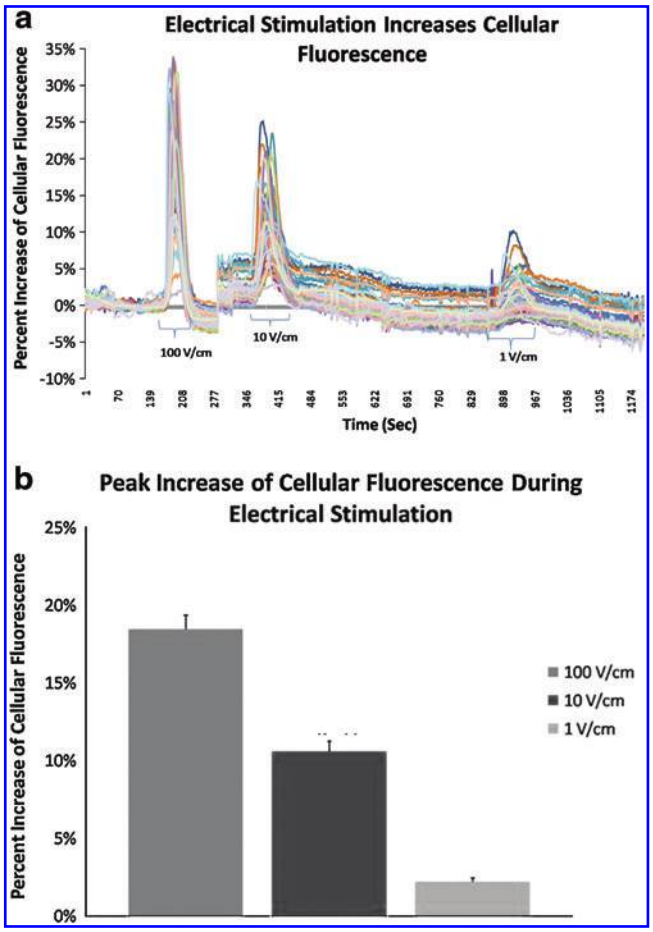

FIG. 7. (**a**) Graphical representation of fluorescence intensities from all cells in the field of view. Electrical stimulation at 10 and 1 V/cm increased cytoplasmic Ca^{2+} after an initial stimulation at 100 V/cm for 5 min. (**b**) Percent increases in cellular fluorescence in three equivalent experiments in which cells were stimulated electrically at 100, 10, and 1 V/cm at 1 Hz for 5 min, in that order. Cells remained as responsive to electric field stimulation after an acute stimulation at 100 V/cm as they were when the order was reversed, that is, from low to high field strength. Color images available online at www.liebertonline.com/ten.

of potentials on the micron scale. Stimulation *in vitro* by capacitative coupling differs from this approach since each element placed between the metal plates fixed to the dish will experience a voltage drop, with the sum of all drops equaling the applied voltage.[26] This is also true for in-solution electrodes spaced macroscopic distances apart or for inductive coupling. Thus, forming a controlled electric field pattern at the location of the cells is difficult to achieve with long distances between the electrodes.

In-solution electrodes, such as salt-based electrodes or metal electrodes, have also been used for exposing cells to electric field treatments. One concern with in-solution electrodes is that, at certain voltages, electrochemical effects due to the reduction or oxidation of salts or other charged additives at reactive metal electrodes can result in electrode fouling. Such electrochemistry is voltage dependent, and thus can be minimized by shrinking feature sizes, which enables use of lower voltages. In our case, the use of IDEs with a small feature size (100 μm) enabled production of a clinically significant electric field with a significantly smaller voltage than in traditional techniques.[3] We point out that feature sizes as small as 10 μm are easily achievable utilizing this technique. In addition, the pattern could be altered (in particular, made more complex), by changing the design of the photolithography mask.

The use of IDEs not only localizes the field to a well-defined region (here, $1\times1\times100$ μm) but that region is also visually accessible for fluorescence-based assays, due to the open nature of the electrode design. In addition, because the electrodes are rigidly placed on a supporting surface, the electrode spacing is precisely and permanently defined, increasing reproducibility. To our knowledge, this IDE configuration has not been widely utilized for electrical stimulation, but our calculations and preliminary data indicate that it should be as effective as more traditional means, with the additional advantages of increased reproducibility, decreased applied voltage, and the ability to easily image the cells under electrical stimulation.

It has been well documented that cells are able to respond to electric stimulation by activation of calcium channels present within the cell membrane and release of calcium from intracellular calcium stores.[27] As we have now shown, hASCs are also able to respond to electric field stimulation by a calcium signaling pathway and, at increasing electric field strength, the calcium response is directly affected. Hammerick *et al.* have also shown that electric fields of 6 V/cm at 50 Hz induced calcium signaling in mouse ASCs.[17] Previous work by Dr. Michael Cho's research group has characterized a myriad of calcium signaling responses to different electric fields for both responsive and unresponsive cell types.[2,3,5,27] Their research has indicated that differing electric field magnitudes and frequencies result in different mechanisms for increased cytosolic Ca^{2+} (i.e., release from intracellular stores or opening of ion channels).[2] Similarly, Li *et al.* have found that ultrasound and pulsed electromagnetic field stimulation are equally effective at increasing osteoblast proliferation, and identified alternative transduction pathways in the two cases, both resulting in an increase in cytosolic Ca^{2+}.[28] Our results indicate that hASCs also respond to electrical stimulation by increasing intracellular calcium.

Long-term regimented exposure to low-frequency electric fields has been viewed as a possible treatment method and therapy to drive osteogenic differentiation. By culturing hASCs in osteogenic differentiating medium containing dexamethasone, β-glycerol phosphate, and ascorbic acid and exposing them to a 1 Hz AC electric field of 1 V/cm, we have shown a significant increase in the amount of mineralized calcium produced relative to unstimulated controls and other physiological field strengths of 3 and 5 V/cm. Mineralized calcium is a late marker of bone differentiation and is often used as a final assessment for bone tissue engineering. Comparative results have been reported by Martino *et al.*, where SaOS-2 cells were cultured in an AC electric field of 9 mV/cm at 15 Hz.[29] They reported no effect on proliferation or increases in alkaline phosphatase activity. However, visual inspection of the cultures demonstrated a large presence of bone-like nodules and the cells produced 2.5× more calcium than unstimulated controls. Sun *et al.* determined that there was no effect on the overall growth rate or morphology of human MSCs (hMSCs) in response to electrical stimulation but that calcium signaling dynamics were altered and

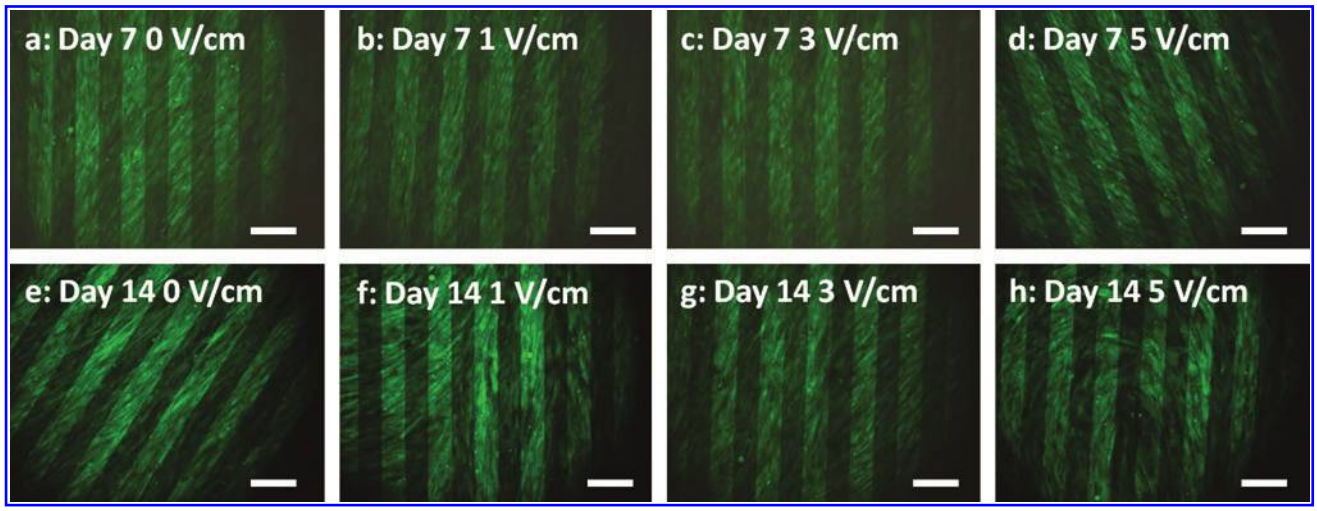

FIG. 8. hASC viability after 7 (**a–d**) and 14 (**e–h**) days of stimulation *in vitro* at 0, 1, 3, or 5 V/cm for 4 h/day. Cells remained viable and grew into a confluent monolayer on top of the interdigitated electrode. Live cells = green; dead cell = red; scale bar = 200 μm. Color images available online at www.liebertonline.com/ten.

osteogenic differentiation enhanced as indicated by increasing collagen I and alkaline phosphatase gene expression.[3] They also found that the amount of mineralized calcium was significantly increased as determined by histological staining. Similar to these previous findings with other stem and progenitor cells, our findings indicate that application of a 1 Hz, 1 V/cm electric field results in >2× the amount of mineral than that produced by unstimulated controls. To reveal possible mechanisms behind electric stimulation, investigators have attempted to assess the mode of interaction between electric fields and cells. Research has investigated the effects of electric stimulation on the mechanical properties of MSCs in an attempt to determine if acute applications could generate significant changes in properties, including cytoskeleton organization and elastic modulus to direct differentiation. A study initiated by Titushkin and Cho investigated the application of a direct current electric field of 2 V/cm for both hMSCs and osteoblasts and determined that after application of the electrical stimulus, there was a significant reduction in the modulus for both cell types.[30,31] This decrease in cell elasticity was due to the substantial reorganization of the actin cytoskeleton. This reorganization has been hypothesized to be based on molecular signaling such as increases in intracellular Ca^{2+} and depletion of intracellular ATP. These signaling processes are attributed to the decrease in the structural properties of hMSCs, making them more similar to fully differentiated osteoblasts.[30] Titushkin and Cho further hypothesized that the reduction in actin organization and membrane tension can then enhance endocytosis and transmembrane movement of soluble osteogenic factors, providing a synergistic inducement toward osteogenic differentiation.

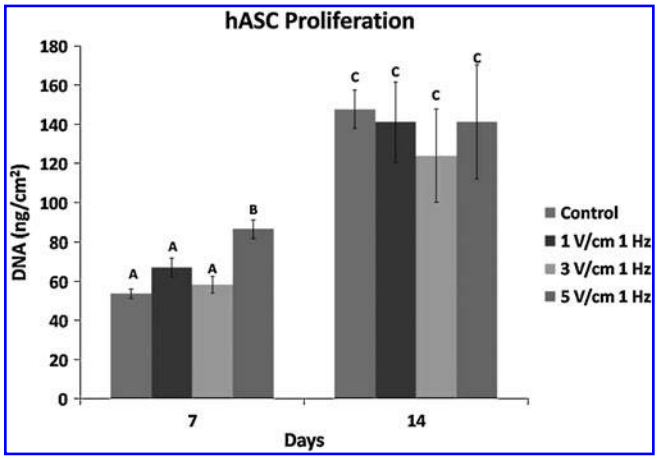

FIG. 9. hASC proliferation after 7 and 14 days *in vitro* with electric field stimulation of 0 (control), 1, 3, or 5 V/cm at 1 Hz for 4 h/day. At day 7, the 5 V/cm treatment (group B) stimulated proliferation to a significantly greater extent ($p < 0.05$) than 0, 1, or 3 V/cm (groups A). By day 14, hASC proliferation was not affected by electric field treatments of 0, 1, 3, or 5 V/cm (groups C). Values of groups not connected by same letter are significantly different ($p < 0.05$).

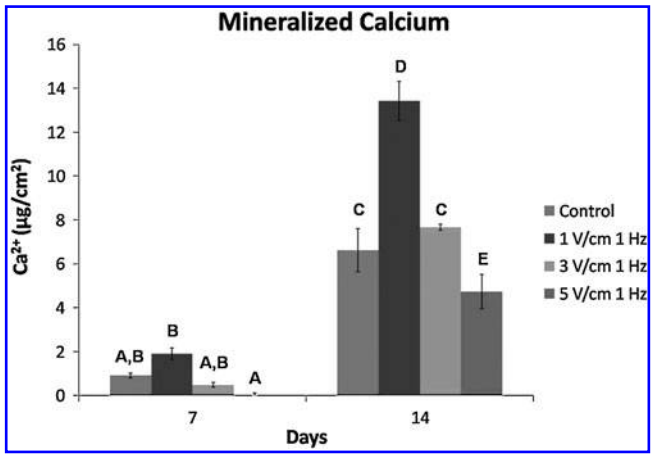

FIG. 10. hASC mineralization was assessed after 7 and 14 days *in vitro* for hASCs exposed to osteogenic supplements (dexamethasone, β-glycerol phosphate, and ascorbic acid) and electric field stimulation of 0 (control), 1, 3, or 5 V/cm at 1 Hz for 4 h/day. At 7 and 14 days, values of groups not connected by same letters are significantly different ($p < 0.05$).

In addition to using electric stimulation for enhancing osteogenesis, other researchers have attempted to determine the effects of electric stimulation on MSCs undergoing adipogenesis. In a recent study, Sun *et al.* assessed the effect of pulsed-electromagnetic fields on hMSC proliferation and differentiation down osteogenic, adipogenic, and neurogenic lineages. The authors reported slight enhancement in cellular proliferation but were unable to determine any significant changes in adipogenic cellular differentiation as determined by Oil Red O.[32]

The use of IDEs in combination with human adipose-derived stem cells provides a facile technique to culture and expose cells to regimented electric field treatments. The injection of charge into our system can be achieved by utilizing either a voltage or current source between the contact pads of the IDEs. As reported in this work and others, we have utilized a voltage source to apply electric stimulation to cells in culture, which is adequate for stimulating hASCs on IDEs and with other electrode designs.[33] Although this method is sufficient for delivering charge to the electrodes, it is limited due to the voltage source only controlling the net potential and not the current in the culture. Our future experiments will focus on recording the induced current over time of culture. Overall, the use of the IDEs allows direct observation of cell signaling pathways using fluorescent microscopy techniques and offers a $1\,cm^2$ footprint to evaluate and characterize extracellular deposited materials.

Conclusions

In this study, the response of hASCs to an applied electric field was investigated utilizing a custom planar IDE configuration along with real-time fluorescence tracking of cytoplasmic Ca^{2+} changes and hASC-mediated mineral deposition. hASCs were responsive to all electric field treatments (1, 3, 5, 10, 100, and 1000 V/cm at 1 Hz) and were able to maintain viability up to at least 100 V/cm. Future experiments will focus on further quantifying the characteristics of induced Ca^{2+} responses, delineating the mechanism(s) by which cytoplasmic Ca^{2+} is increased in hASCs by electrical stimulation, and identifying the underlying mechanism(s) that link changes in intracellular Ca^{2+} with the increased osteodifferentiation potential of hASCs when subjected to electric field stimulation. Our studies have demonstrated that electrical stimulation of hASCs with IDEs is an effective approach, in addition to having several special technical advantages with respect to other methods that make this a valuable system for further study.

Acknowledgments

This project was supported by Award Number UL1RR025747 from the National Center for Research Resources (E.G.L.). The authors would like to thank Adisri Charoenpanich for her excellent technical assistance.

Disclosure Statement

No competing financial interests exist.

References

1. Voldman, J. Electrical forces for microscale cell manipulation. Annual Review of Biomedical Engineering (8), 425–454, 2006.
2. Khatib, L., Golan, D.E., and Cho, M.R. Physiologic electrical stimulation provokes intracellular calcium increase mediated by phospholipase C activation in human osteoblasts. FASEB J **18,** 1903, 2004.
3. Sun, S., Liu, Y., Lipsky, S., and Cho, M. Physical manipulation of calcium oscillations facilitates osteodifferentiation of human mesenchymal stem cells. FASEB J **21,** 1472, 2007.
4. Levin, M. Bioelectromagnetics in morphogenesis. Bioelectromagnetics **24,** 295, 2003.
5. Sun, S., Titushkin, I., and Cho, M. Regulation of mesenchymal stem cell adhesion and orientation in 3D collagen scaffold by electrical stimulus. Bioelectrochemistry **69,** 133, 2006.
6. Lavine, L.S., and Grodzinsky, A.J. Electrical-stimulation of repair of bone. J Bone Joint Surg Am **69A,** 626, 1987.
7. Whitehead, M.A., Fan, D., Akkaraju, G.R., Canha, M.L.T., and Coffer, J.L. Accelerated calcification in electrically conductive polymer composites comprised of poly(epsilon-caprolactone), polyaniline, and bioactive mesoporous silicon. J Biomed Mater Res Part A **83A,** 225, 2007.
8. Brighton, C.T., Wang, W., Seldes, R., Zhang, G.H., and Pollack, S.R. Signal transduction in electrically stimulated bone cells. J Bone Joint Surg Am **83A,** 1514, 2001.
9. Wang, Q., Zhong, S., Ouyang, J., Jiang, L., Zhang, Z., Xie, Y., and Luo, S.Q. Osteogenesis of electrically stimulated bone cells mediated in part by calcium ions. Clin Orthop 259, 1998.
10. Spadaro, J.A. Mechanical and electrical interactions in bone remodeling. Bioelectromagnetics **18,** 193, 1997.
11. Piacentini, R., Ripoli, C., Mezzogori, D., Azzena, G.B., and Grassi, C. Extremely low-frequency electromagnetic fields promote *in vitro* neurogenesis via upregulation of ca(v)1-channel activity. J Cell Physiol **215,** 129, 2008.
12. Haddad, J.B., Obolensky, A.G., and Shinnick, P. The biologic effects and the therapeutic mechanism of action of electric and electromagnetic field stimulation on bone and cartilage: new findings and a review of earlier work. J Altern Complement Med **13,** 485, 2007.
13. Pittenger, M.F., Mackay, A.M., and Beck, S.C. Multilineage potential of adult human mesenchymal stem cells. Science **284,** 143, 1999.
14. Zuk, P.A., Zhu, M., Mizuno, H., Huang, J., Futrell, J.W., Katz, A.J., Benhaim, P., Lorenz, H.P., and Hedrick, M.H. Multilineage cells from human adipose tissue: implications for cell-based therapies. Tissue Eng **7,** 211, 2001.
15. De Ugarte, D.A., Morizono, K., Elbarbary, A., Alfonso, Z., Zuk, P.A., Zhu, M., Dragoo, J.L., Ashjian, P., Thomas, B., Benhaim, P., Chen, I., Fraser, J., and Hedrick, M.H. Comparison of multi-lineage cells from human adipose tissue and bone marrow. Cells Tissues Organs **174,** 101, 2003.
16. Gimble, J.M., Katz, A.J., and Bunnell, B.A. Adipose-derived stem cells for regenerative medicine. Circ Res **100,** 1249, 2007.
17. Hammerick, K., James, A., Huang, Z., Prinz, F., and Longaker, M. Pulsed DC electric fields enhance osteogenesis in adipose-derived stromal cells. Tissue Eng Part A **16,** 917, 2010.
18. Aaron, R.K., and Ciombor, D.M. Acceleration of experimental endochondral ossification by biophysical stimulation of the progenitor cell pool. J Orthop Res **14,** 582, 1996.
19. Aaron, R.K., Ciombor, D.M., and Simon, B.J. Treatment of nonunions with electric and electromagnetic fields. Clin Orthop (419), 21, 2004.
20. Wiesmann, H.P., Hartig, M., Stratmann, U., Meyer, U., and Joos, U. Electrical stimulation influences mineral formation of osteoblast-like cells *in vitro*. Biochim Biophys Acta Mol Cell Res **1538,** 28, 2001.

21. Supronowicz, P.R., Ajayan, P.M., Ullmann, K.R., Arulanandam, B.P., Metzger, D.W., and Bizios, R. Novel current-conducting composite substrates for exposing osteoblasts to alternating current stimulation. J Biomed Mater Res **59,** 499, 2002.
22. Sebastian, A., Venkatesh, A.G., and Markx, G.H. Tissue engineering with electric fields: investigation of the shape of mammalian cell aggregates formed at interdigitated oppositely castellated electrodes. Electrophoresis **28,** 3821, 2007.
23. den Otter, M. Approximate expressions for the capacitance and electrostatic potential of interdigitated electrodes. Sens Actuators **A96,** 140, 2002.
24. Wall, M.E., Bernacki, S.H., and Loboa, E.G. Effects of serial passaging on the adipogenic and osteogenic differentiation potential of adipose-derived human mesenchymal stem cells. Tissue Eng **13,** 1291, 2007.
25. Crew, N., Darabi, J., Voglewede, P., Guo, F., and Bayoumi, A. An analysis of interdigitated electrode geometry for dielectrophoretic particle transport in micro-fluidics. Sens Actuators B **125,** 672, 2007.
26. Aaron, R.K., Ciombor, D.M., Wang, S., and Simon, B. Clinical biophysics: the promotion of skeletal repair by physical forces. Skeletal Dev Remodel Health Dis Aging **1068,** 513, 2006.
27. Titushkin, I.A., Rao, V.S., and Cho, M.R. Mode- and cell-type dependent calcium responses induced by electrical stimulus. IEEE Trans Plasma Sci **32,** 1614, 2004.
28. Li, J.K.J., Lin, J.C.A., Liu, H.C., Sun, J.S., Ruaan, R.C., Shih, C., and Chang, W.H.S. Comparison of ultrasound and electromagnetic field effects on osteoblast growth. Ultrasound Med Biol **32,** 769, 2006.
29. Martino, C.F., Belchenko, D., Ferguson, V., Nielsen-Preiss, S., and Qi, H.J. The effects of pulsed electromagnetic fields on the cellular activity of SaOS-2 cells. Bioelectromagnetics **29,** 125, 2008.
30. Titushkin, I.A., and Cho, M. Modulation of cellular mechanics during osteogenic differentiation of human mesenchymal stem cells. Biophys J **93,** 3693, 2007.
31. Titushkin, I.A., and Cho, M. Regulation of cell cytoskeleton and membrane mechanics by electric field: role of linker proteins. Biophys J **96,** 717, 2009.
32. Sun, L.Y., Hsieh, D.K., Yu, T.C., Chiu, H.T., Lu, S.F., Luo, G.H., Kuo, T.K., Lee, O.K., and Chiou, T.W. Effect of pulsed electromagnetic field on the proliferation and differentiation potential of human bone marrow mesenchymal stem cells. Bioelectromagnetics **30,** 251, 2009.
33. Tandon, N., Cannizzaro, C., Chao, P.H., Maidhof, R., Marsano, A., Au, H.T.H., Radisic, M., and Vunjak-Novakovic, G. Electrical stimulation systems for cardiac tissue engineering. Nat Protoc **4,** 155, 2009.

Address correspondence to:
Elizabeth G. Loboa, Ph.D.
Joint Department of Biomedical Engineering at the University of North Carolina at Chapel Hill and North Carolina State University
2142 Burlington Laboratories
Campus Box 7115
Raleigh, NC 27695-7115

E-mail: egloboa@ncsu.edu

Received: November 19, 2009
Accepted: March 29, 2010
Online Publication Date: April 27, 2010

This article has been cited by:

1. Georgina To###a Salazar, Osamu Ohneda. 2012. Review of biophysical factors affecting osteogenic differentiation of human adult adipose-derived stem cells. *Biophysical Reviews* . [CrossRef]
2. Sneha Agarwal, Anil Sebastian, Lesley M. Forrester, Gerard H. Markx. 2012. Formation of embryoid bodies using dielectrophoresis. *Biomicrofluidics* **6**:2, 024101. [CrossRef]
3. L. Tirkkonen, H. Halonen, J. Hyttinen, H. Kuokkanen, H. Sievanen, A.-M. Koivisto, B. Mannerstrom, G. K. B. Sandor, R. Suuronen, S. Miettinen, S. Haimi. 2011. The effects of vibration loading on adipose stem cell number, viability and differentiation towards bone-forming cells. *Journal of The Royal Society Interface* **8**:65, 1736-1747. [CrossRef]
4. Akon Higuchi , Po-Yen Shen , Jun-Kai Zhao , Ching-Wen Chen , Qing-Dong Ling , Hui Chen , Han-Chow Wang , Jun-Tang Bing , Shih-Tien Hsu . 2011. Osteoblast Differentiation of Amniotic Fluid-Derived Stem Cells Irradiated with Visible Light. *Tissue Engineering Part A* **17**:21-22, 2593-2602. [Abstract] [Full Text HTML] [Full Text PDF] [Full Text PDF with Links]
5. Yongsung Hwang, Ameya Phadke, Shyni Varghese. 2011. Engineered microenvironments for self-renewal and musculoskeletal differentiation of stem cells. *Regenerative Medicine* **6**:4, 505-524. [CrossRef]
6. Josephine C. Bodle , Ariel D. Hanson , Elizabeth G. Loboa . 2011. Adipose-Derived Stem Cells in Functional Bone Tissue Engineering: Lessons from Bone Mechanobiology. *Tissue Engineering Part B: Reviews* **17**:3, 195-211. [Abstract] [Full Text HTML] [Full Text PDF] [Full Text PDF with Links]